Research Square

Preprints are preliminary reports that have not undergone peer review.
They should not be considered conclusive, used to inform clinical practice,
or referenced by the media as validated information.

Preparation and Performance of a Multifunctional Acid Thickener for High-Temperature Carbonate Acidizing

Xinghua Zhang
Tianjin Company, CNOOC (China)
Xuxing Wang
China Oilfield Services Limited
Wanwan Li
China Oilfield Services Limited
Kechao Gao
Tianjin Company, CNOOC (China)
Guangfeng Chen
Tianjin Company, CNOOC (China)
Wenlong Zhang
275623526@qq.com

Changzhou University

Research Article

Keywords: Multifunctional thickener, gelled acid, crosslinked acid, diverting acid

Posted Date: November 10th, 2026

DOI: https://doi.org/10.21203/rs.3.rs-11401217/v1

License: This work is licensed under a Creative Commons Attribution 4.0 International License.
Read Full License

Additional Declarations: No competing interests reported.

Preparation and Performance of a Multifunctional Acid Thickener for High-Temperature Carbonate Acidizing

Xinghua Zhang [1]; Xuxing Wang [2]; Wanwan Li [2]; Kechao Gao [1]; Guangfeng Chen [1]; Wenlong Zhang [3]

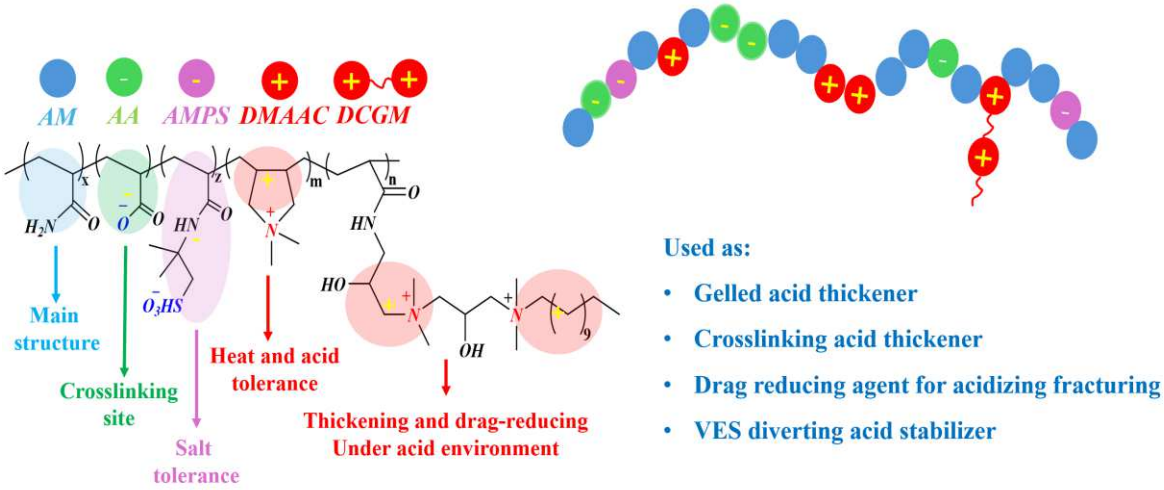
[1] Tianjin Company, CNOOC (China), Tianjin 300452, China

[2] China Oilfield Services Limited, Tianjin 300452, China

[3] Changzhou University, School of Petrochemical Engineering, Changzhou, Jiangsu, 213164, China

Corresponding author: Wenlong Zhang

Email: 275623526@qq.com



Abstract: To address the single functionality, insufficient temperature and acid resistance, and difficulty in balancing retardation and diversion of acidizing fluids for high-temperature carbonate reservoirs, a zwitterionic penta-copolymer hydrophobic associating thickener (MFAT) was designed and synthesized. Its backbone contains amide, carboxyl, and sulfonic groups, while its hydrophobic and cationic side chains contain numerous quaternary ammonium cations and di-cationic structures, enabling good molecular chain extension, hydrophobic association, and electrostatic synergy in strongly acidic and high-ionic-strength environments. MFAT has a viscosity-average molecular weight of 8.43×10^6 g/mol and shows good thickening ability in 20% HCl as a gelled acid thickener. With viscoelastic surfactants, it forms a high-temperature-resistant gelled acid system with a retardation rate above 65% at 160 °C. MFAT and organic zirconium crosslinker construct a delayed crosslinked acid system with a crosslinking time of up to 157 s and a retardation rate above 75% at 160 °C. In 20%

HCl, 0.2% MFAT exhibits the best drag reduction performance, and with surfactant assistance, the drag reduction rate exceeds 75%. Additionally, 0.1% MFAT significantly improves the temperature resistance of VES diverting acid; parallel core experiments show the maximum temporary plugging diversion pressure increases from 3.9 to 5.3 MPa, and the permeability improvement ratio of the low-permeability core increases from 8.53 to 12.63. These results indicate that MFAT constructs an acid- and temperature-resistant associating network through the synergy of "hydrophobic association–electrostatic interaction–hydrogen bonding," serving as a multifunctional acidizing thickener for gelled acid, crosslinked acid, drag-reducing acid, and diverting acid systems in high-temperature carbonate acidizing, with important engineering application value.

Keywords: Multifunctional thickener; gelled acid; crosslinked acid; diverting acid

1. Introduction

In carbonate acidizing, the reaction rate between the acid fluid and the rock is one of the key factors determining the acidizing effect [1-3]. For high-temperature and high-pressure carbonate reservoirs, conventional hydrochloric acid reacts extremely rapidly with carbonate rock, and the acid is often consumed near the wellbore, resulting in a limited acid-etched fracture length and making deep penetration into distant fractures difficult [4, 5]. To solve this problem, the viscosity of the acid fluid usually needs to be increased to inhibit the mass transfer of H^+ to the rock surface, reduce the acid–rock reaction rate, and thereby achieve deep acid penetration [1-6]. Gelled acid and crosslinked acid are two commonly used high-temperature acidizing systems. Gelled acid increases the acid viscosity through a thickener, reduces the hydrogen ion mass transfer rate, and thus retards the acid–rock reaction [6, 7]. Crosslinked acid, on the other hand, forms a three-dimensional gel network in a strongly acidic environment through a thickener and an organic crosslinker, further improving the acid viscosity and retardation performance, and therefore has good application prospects in high-temperature carbonate acid fracturing [8-11]. In addition, for relatively low-temperature or unconventional oil and gas reservoirs, large-displacement slickwater acid systems are often used for volumetric fracture network construction, which places higher demands on acid-resistant drag reducers [12, 13]. For porous carbonate rocks, viscoelastic surfactant (VES) diverting acid is an effective matrix acidizing fluid. It preferentially enters high-permeability macropores, thickens as the acid–rock reaction proceeds, and

plugs the macropores, forcing subsequent acid to enter low-permeability regions and achieving acid diversion [14-18]. However, VES diverting acid is mainly composed of small-molecule surfactants. At high temperatures ($>120°C$), intensified molecular thermal motion and decreased micelle structural stability lead to insufficient temperature resistance and diversion performance [19, 20].

It can thus be seen that high-temperature carbonate acidizing often requires the separate development of thickeners, crosslinkers, drag reducers, and stabilizers, resulting in complex systems, high compatibility requirements, and inconvenient field application. At present, research on acid thickeners at home and abroad mainly focuses on polyacrylamides, sulfonic acid polymers, hydrophobic associating polymers, and zwitterionic polymers. Although polyacrylamide thickeners have good thickening ability, they are prone to acid-induced hydrolysis and thermal degradation under strongly acidic and high-temperature conditions, leading to viscosity loss [3-9, 19, 20]. Sulfonic acid polymers, owing to the introduction of strongly acidic monomers such as AMPS, show improved acid and salt resistance, but their drag reduction and diversion stabilization functions are limited. Hydrophobic associating polymers form reversible networks through physical association between hydrophobic chains and exhibit good thickening and shear resistance, but in strongly acidic and high-ionic-strength environments, hydrophobic association is easily affected by ionic shielding and acid-induced chain coiling. Zwitterionic polymers, because they contain both cationic and anionic groups, have good salt tolerance and anti-polyelectrolyte effects, and show potential application advantages in strongly acidic environments. However, research on multifunctional acid thickeners that simultaneously possess thickening, drag reduction, crosslinking, and VES stabilization functions is still relatively scarce, especially systematic evaluations under high-temperature carbonate acidizing conditions [21, 22].

Based on the above problems, this work designed and synthesized a zwitterionic penta-copolymer hydrophobic associating polymer thickener (MFAT), in which cationic groups, sulfonic groups, and long hydrophobic chains are simultaneously introduced into the molecular structure. Among them, AM provides the backbone skeleton and hydrogen bonding sites; AA provides carboxyl groups, enhancing the hydrophilicity and pH responsiveness of the molecular chain; AMPS provides strongly acidic sulfonic groups, enabling the polymer to maintain certain charge repulsion and chain extension ability in strongly acidic and high-salt environments; DMDAAC and DCGM provide cationic groups and long hydrophobic chains. In particular, DCGM contains a di-

cationic structure and long-chain alkyl groups, enabling it to form a physical crosslinking network through the synergy of electrostatic interaction [18-22], hydrophobic association, and hydrogen bonding even under strongly acidic conditions. This structure allows MFAT to maintain good thickening, drag reduction, and stabilization abilities in strongly acidic and high-ionic-strength environments. MFAT can be used not only as a thickener for preparing gelled acid or crosslinked acid, but also for achieving drag reduction in strongly acidic environments, and as a stabilizer for VES diverting acid to improve its temperature resistance.

In this work, the molecular structure, viscosity-average molecular weight, critical association concentration, rheological properties, temperature and shear resistance, retardation performance, crosslinking characteristics, drag reduction performance, and diverting acidizing effect of MFAT were systematically studied, and its mechanism of action was analyzed. The results can provide a theoretical basis and experimental support for the design of multifunctional acidizing fluids for high-temperature carbonate reservoirs, and have important engineering significance for simplifying acid fluid formulations and improving the comprehensive performance of high-temperature acidizing fluids.

2. Experimental

2.1 Materials

Acrylamide (AM), acrylic acid (AA), 2-acrylamido-2-methylpropanesulfonic acid (AMPS), dimethyldiallylammonium chloride (DMDAAC), dodecylamine, epichlorohydrin, and N-(3-dimethylaminopropyl)methacrylamide (DMAPMA) were all of analytical grade and purchased from Shanghai Aladdin Biochemical Technology Co., Ltd. Ethanol, hydrochloric acid, ethyl acetate, sodium hydroxide, and 2,2'-azobis(2-methylpropionamidine) dihydrochloride (V_{50}) were all of analytical grade and purchased from Shanghai Macklin Biochemical Technology Co., Ltd. Rock slices and cores were made of artificial carbonate material. Erucylamide propyl dimethylamine carboxybetaine (EDCB) and erucylamide propyl dimethylamine sulfobetaine (EDSB) were of industrial grade and purchased from Shanghai Yincong New Material Co., Ltd. VES self-diverting acid agent (SDA) and organic zirconium crosslinker for crosslinked acid were of industrial grade and purchased from Sichuan Annengjie Technology Co., Ltd.

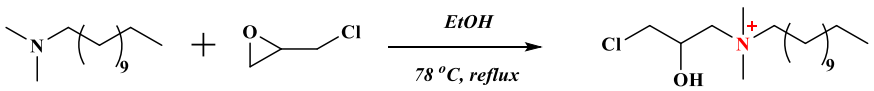
2.2 Methods

2.2.1 Synthesis

(1) Synthesis of hydrophobic monomer

Synthesis of intermediate

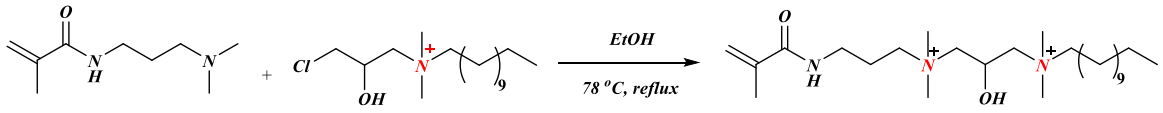
In a 500 mL round-bottom flask, dodecylamine (200 mmol, 37.08 g) and epichlorohydrin (200 mmol, 18.5 g) were dissolved in 200 mLethanol. The flask was placed in an oil bath and reacted at 78°Cunder magnetic stirring and reflux for 18 h. After the reaction, the solvent was removed using a vacuum rotary evaporator at 60°C, and the product was recrystallized three times in ethyl acetate at 0°Cto obtain a relatively pure intermediate. The synthetic route of the intermediate is shown in ***Scheme 1***.



Scheme 1. Synthetic route of the intermediate

Synthesis of DCGM

In a 500 mL round-bottom flask, N-(3-dimethylaminopropyl) methacrylamide (DMAPMA, 100 mmol) and the above intermediate (100 mmol) were dissolved in 200 mLethanol. The flask was placed in an oil bath and reacted at 65°Cunder magnetic stirring and reflux for 12 h. After the reaction, the solvent was removed using a vacuum rotary evaporator at 60°C, and the product was recrystallized three times in ethyl acetate at 0°C to obtain a relatively pure dicationic group monomer (DCGM). The synthetic route of DCGM is shown in ***Scheme 2***.

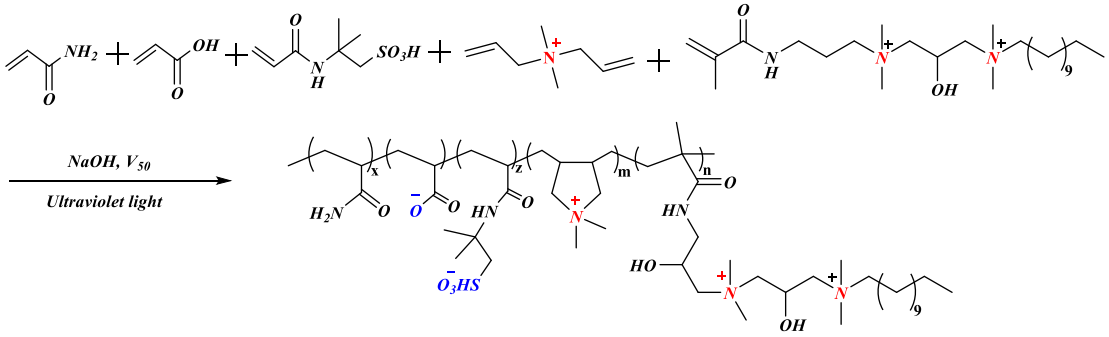


Scheme 2. Synthetic route of the dicationic group monomer (DCGM)

(2) Synthesis of polymer

Using deionized water as solvent, AM, AA, AMPS, DMDAAC, and DCGM were formulated into an aqueous solution with a mass concentration of 30 wt% at a molar ratio of 20: 3: 5: 8: 1, and the pH was adjusted to 7 with NaOH solution. Subsequently, urea was added as a stabilizer and stirred to dissolve completely. The reaction system was purged with nitrogen for 30 min to remove dissolved oxygen, and then V_{50} was added as an initiator. The polymerization reaction was carried out at room temperature under ultraviolet light irradiation. After several hours, a gel-like polymer product was obtained. The polymerization process is shown in ***Scheme 3***.

After solution polymerization was completed, the obtained gel-like polymer block was cut into small particles and washed 2~3 times with anhydrous ethanol to remove unreacted monomers and by-products. The purified polymer particles were transferred to a culture dish and dried in an oven at $50°C$ for 24 h. Finally, the dried polymer particles were ground and sieved to obtain a fine polymer powder with a uniform particle size distribution.



Scheme 3. Synthetic route of the multifunctional acid thickener (MFAT)

2.2.2 Molecular structure characterization

The molecular structures of the synthesized compounds were characterized using a Bruker AVANCE III HD 400 nuclear magnetic resonance spectrometer (Bruker, Karlsruhe, Germany). During ^{1}H NMR sample preparation, the dicationic group monomer (DCGM) was dissolved in deuterated chloroform, and the multifunctional acid thickener (MFAT) was dissolved in deuterated water.

2.2.3 Viscosity-average molecular weight (M_v)

The viscosity-average molecular weight (M_v) of the polymer was determined using an Ubbelohde viscometer (Schott Instruments, Mainz, Germany). First, a polymer stock solution with an initial concentration of 1000 mg/L (C_0) was prepared and then diluted stepwise to obtain five polymer solutions of different concentrations. At $25 \pm 0.1°C$, the efflux time (t) of each solution through the viscometer was measured. A 1 mol/L NaCl solution was used as a reference, and its efflux time (t_0) was measured. The relative viscosity (η_r) and specific viscosity (η_{sp}) were calculated according to ***Eq.* (1).** [23, 24]

$$\eta_{sp} = \frac{t - t_0}{t_0} = \eta_r - 1 \qquad (1)$$

With C_r as the abscissa and η_{sp}/C_r and $\ln[\eta_r/C_r]$ as the ordinates, the two extrapolated lines were plotted, and the intercept on the ordinate axis at the intersection of the two lines was recorded as H. The viscosity-average molecular weight (M_v) of

the polymer was calculated according to ***Eqs.* (2) and (3)** [23, 24].

$$[\eta] = H/C_0 \qquad (2)$$

$$M_v = 802[\eta]^{1.25} \qquad (3)$$

2.2.4 Apparent viscosity

The apparent viscosity of the samples was determined using a six-speed rotational viscometer (NDJ-95A, Shanghai Precision & Scientific Instrument Co., Ltd., China). The measurement was performed at a shear rate of 170 s^{-1}, corresponding to a rotational speed of 100 rpm. The apparent viscosity was calculated according to Eq. (4) [25, 26].

$$\eta = \frac{0.511\theta}{1.703 \times 100} \times 1000 = 3\theta \qquad (4)$$

where η is the apparent viscosity, mPa · s; $\theta$is the dial reading.

2.2.5 Viscoelasticity test

The viscoelastic properties of the samples were evaluated by oscillatory measurements using a rotational rheometer (MCR 301, Anton Paar, Austria). Frequency sweeps were performed in the linear viscoelastic region from 0.01 to 100 Hz; the linear viscoelastic region was determined by preliminary amplitude sweep tests.

2.2.6 Thixotropy test

The thixotropic properties of the samples were characterized using a rotational rheometer (MCR 301, Anton Paar, Austria) equipped with a PP50 measuring system at 25 ± 0.1°C. A three-stage shear rate protocol was adopted: (a) linear increase from 0 to 100 s^{-1} over 10 min; (b) constant shear at 0 $s^{-1}$for 3 min; and (c) linear decrease from 100 to 0 s^{-1} over 10 min [23].

2.2.7 Temperature and shear resistance test

Temperature and shear resistance tests were conducted using a HAAKE MAR III RS 600 rheometer (Thermo Scientific, Germany) equipped with a high-temperature and high-pressure sealed cell. The test temperature was set at 160°C, and the shear rate was set at 170 s^{-1}. The heating and shearing process lasted for 120 min to evaluate the temperature and shear resistance of the acid fluid system.

2.2.8 Drag reduction rate test

The drag reduction performance of the drag reducer was evaluated by measuring the pressure differentials of water and slickwater under controlled shear conditions. The drag reduction rate (*DR*) was calculated according to ***Eq.* (7).**

$$DR = \frac{\Delta P_1 - \Delta P_2}{\Delta P_1} \times 100\% \qquad (7)$$

where ΔP_1 and ΔP_2 represent the pressure differentials of water and slickwater, respectively, Pa.

2.2.9 Retardation effect evaluation

A carbonate rock sample was weighed (m_1), and its surface area S was calculated. The rock sample was reacted with acid in a high-temperature and high-pressure autoclave for 1 h. After the reaction, the rock sample was washed and dried at $105°C$ for 2 h, and the residual mass (m_2) was weighed. The dissolution rate (v_a) was calculated according to ***Eq.* (8)**, and the retardation rate K was calculated by comparison with the blank hydrochloric acid dissolution rate v_0 according to ***Eq.* (9)**:

$$v_a = \frac{m_1 - m_2}{S \cdot \Delta t} \qquad (8)$$

$$K = \frac{v_0 - v_a}{v_0} \times 100\% \qquad (9)$$

where m_1 is the mass of the rock sample before dissolution, g; m_1 is the mass of the rock sample after dissolution, g; S is the surface area of the rock sample, cm^2; Δt is the dissolution time, h; v_0 is the dissolution rate of the rock sample in 20% HCl, $g \cdot cm^{-2} \cdot h^{-1}$; and v_a is the dissolution rate of the rock sample in the formulated acid fluid, $g \cdot cm^{-2} \cdot h^{-1}$.

2.2.10 Viscosity-variation performance evaluation

A diverting acid with a hydrochloric acid concentration of 20% was prepared, and HCl was consumed by quantitatively adding $Ca(OH)_2$ powder. As HCl was gradually consumed, the apparent viscosity of the spent acid at different residual acid concentrations was measured under a shear rate of 170 s^{-1} to evaluate the viscosity-variation behavior of the diverting acid.

2.2.11 Parallel core experiment

Parallel core experiments were used to evaluate the acidizing diversion effect of the diverting acid. Two carbonate cores with a large permeability contrast were selected for the experiment to simulate formation heterogeneity. Conventional hydrochloric acid, gelled acid, and self-diverting acids with different formulations were used in parallel core displacement experiments. The breakthrough pressure during the displacement process and the permeability contrast of the cores before and after acidizing were recorded to evaluate the diversion acidizing effect.

3 Results and Discussion

3.1 Molecular structure characterization

The ^{1}H NMR spectrum of DCGM is shown in **Fig. 1**. ^{1}H NMR (400 MHz, $CDCl_3$), δ/ppm: 0.86 (t, 3H, $\mathbf{CH_3}CH_2$), 1.31 (m, 20H, $CH_3(\boldsymbol{CH_2})_{10}CH_2$), 1.63 (s, 3H, CH_2=C($\boldsymbol{CH_3}$)C=O), 2.13 (m, 2H, $NHCH_2\boldsymbol{CH_2}CH_2N^+$)，2.25 (t, 2H, O=CNH$\boldsymbol{CH_2}$), 3.24 (s, 12H, $2N^+(\boldsymbol{CH_3})_2$), 3.55 (s, 4H, $2N^+\boldsymbol{CH_2}$), 3.68 (s, 4H, $N^+\boldsymbol{CH_2}CH(OH)\boldsymbol{CH_2}N^+$), 4.13 (m, 1H, ***OH***), 4.32 (s, 1H, $CH_2\boldsymbol{CH}(OH)CH_2$), 5.36 (t, 1H, ***CH***=C), 5.55 (t, 1H, ***CH***=C), 7.83 (s, 1H, CO***NH***).

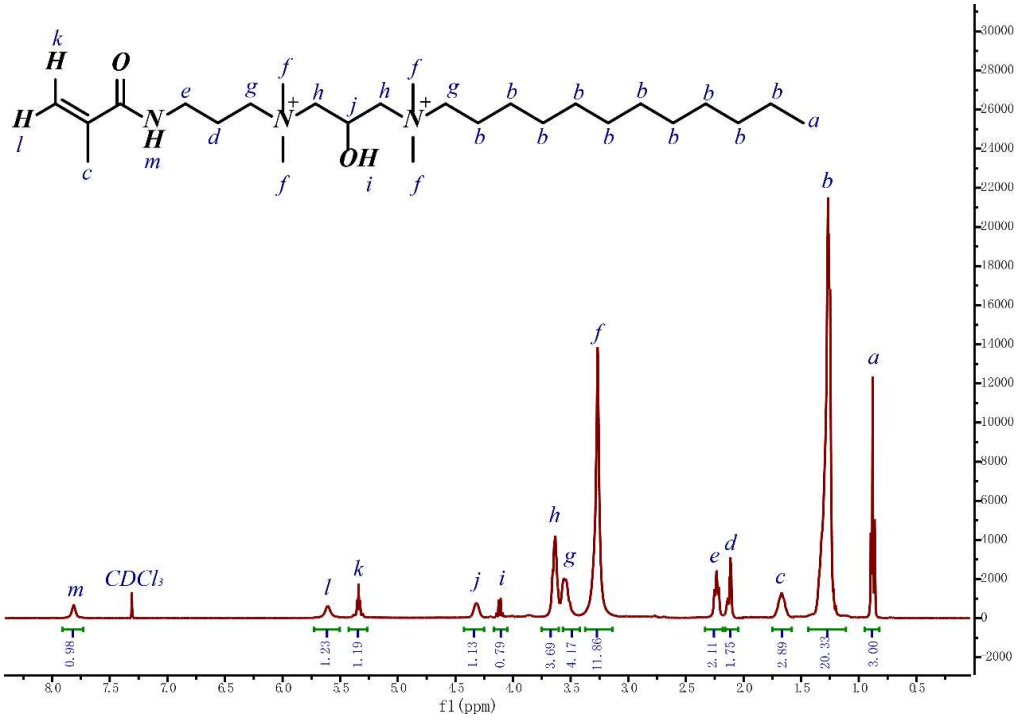


Fig. 1 ^{1}H NMR spectrum of the synthesized monomer DCGM

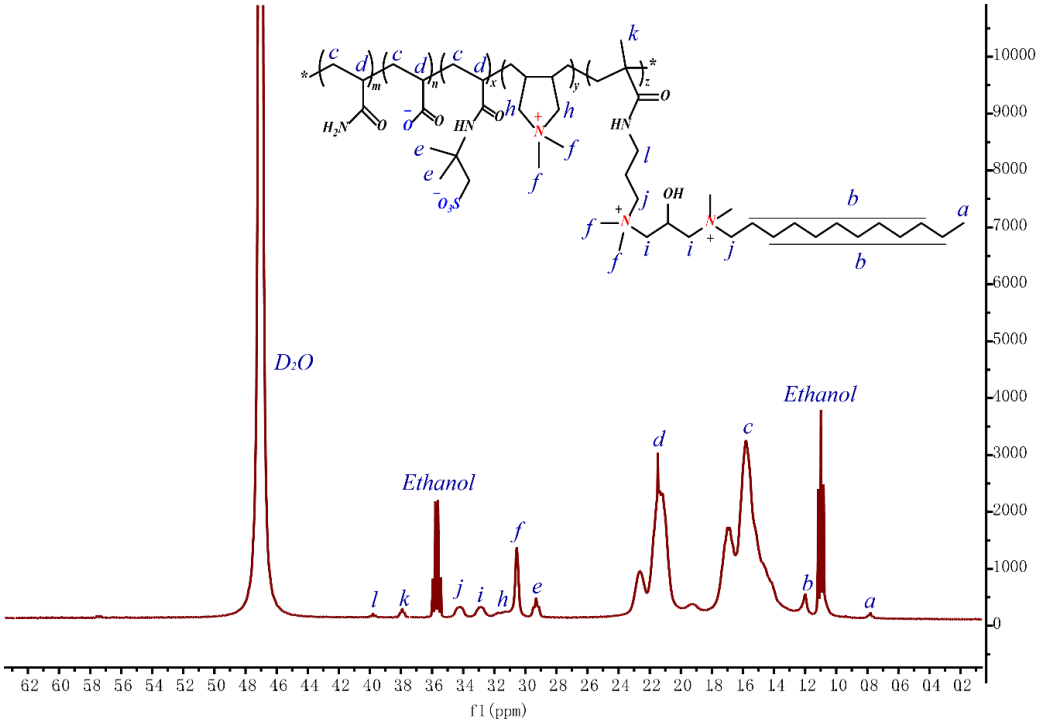


Fig. 2 ^{1}HNMR spectrum of MFAT

The ^{1}H NMR spectrum of MFAT is shown in **Fig. 2**. ^{1}H NMR (400 MHz, D_2O), δ/ppm: 0.86 (s, $N^+CH_2(CH_2)_{10}\boldsymbol{CH_3}$), 1.06 (t, $N^+CH_2\boldsymbol{(CH_2)_{10}}CH_3$), 1.52 (m, -$\boldsymbol{CH_2}$-CH-), 2.11 (m, -$\boldsymbol{CH_2}$-CH-), 2.93 (t, $C(CH_2)_2\boldsymbol{(CH_3)_2}$), 3.04 (s, $N^+\boldsymbol{(CH_3)_2}$), 3.13 (m, $N^+\boldsymbol{(CH_2)_2}$), 3.25 (s, $CH\boldsymbol{(CH_2)_2}OH$), 3.42 (s, $CH_2\boldsymbol{CH_2}N^+$), 3.78 (s, -CH_2-C($\boldsymbol{CH_3}$)-), 3.97 (s, $CONH\boldsymbol{CH_2}$).

3.2 Viscosity-average molecular weight test

Using 1 mol/L NaCl solution as solvent, MFAT polymer solutions with concentrations of 500, 400, 300, 200, and 100 mg/L were prepared. At room temperature, the efflux time of the polymer solution through the Ubbelohde viscometer was measured three times continuously, and the average value was taken. The efflux time of the 1 mol/L NaCl solution through the Ubbelohde viscometer was measured in the same way as a reference. With C_r as the abscissa and η_{sp}/C_r and $\ln(\eta_r/C_r)$ as the ordinates, the results are shown in **Fig. 3**. The two sets of data points were fitted as straight lines, and the intersection of the two lines was extrapolated to the ordinate axis to obtain the intercept H.

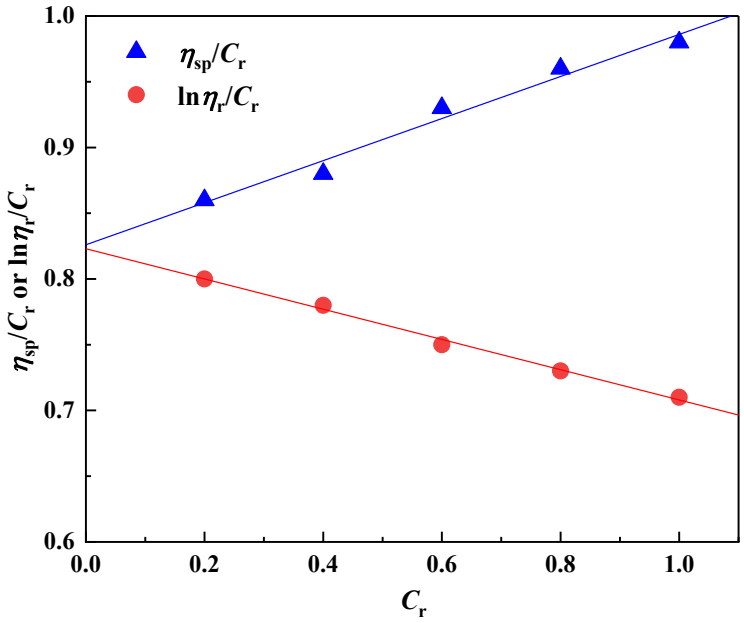


Fig. 3 Determination of viscosity-average molecular weight

Based on the obtained intrinsic viscosity $[\eta]$, the viscosity-average molecular weight of the polymer was calculated using the Mark–Houwink equation, and the results are listed in **Table 1.**

Table 1. Results of polymer molecular weight determination

Polymer	H	$[\eta]$ (mL/g)	M
MFAT	0.825	1650	8.43×10^6

As shown in **Table 1**, the intrinsic viscosity of MFAT is 1650 mL/g corresponding to a viscosity-average molecular weight of 8.43×10^6 g/mol. The relatively high molecular weight indicates that the MFAT backbone has long chain segments and high chain entanglement ability, which is the structural basis for forming an effective thickening network in acid fluids. At the same time, the cationic groups, sulfonic groups, and long hydrophobic chains introduced into the MFAT molecular chain can enhance the electrostatic interaction and hydrophobic association between molecular chains, enabling it to maintain a relatively high hydrodynamic volume and net-work structural stability in strongly acidic environments.

3.3 Critical association concentration

MFAT is a hydrophobic associating polymer, and its intermolecular association ability in aqueous solution directly affects its thickening performance and acid resistance. To study the association behavior of MFAT in different environments, its

critical association concentrations in pure water, strong acid, and surfactant-assisted environments were measured.

As shown in **Fig. 4(a)**, the first critical association concentration of MFAT in pure water is 1444.2 mg/L , and the second critical association concentration is 2406.1 mg/L . The first critical association concentration corresponds to the concentration at which intermolecular hydrophobic association begins to form, and the second critical association concentration corresponds to the concentration at which a denser three-dimensional network structure forms. As shown in **Fig. 4(b)**, in 20 wt% HCl, the first critical association concentration of MFAT decreases to 1154.1 mg/L , and the second critical association concentration decreases to 2269.1 mg/L. This phenomenon indicates that the strongly acidic environment does not weaken the association ability of MFAT, but instead promotes intermolecular association. The reason is that the MFAT molecular chain contains a large number of cationic groups. In a strongly acidic and high-ionic-strength environment, the electrostatic shielding between cationic groups and Cl^- and acid radical ions partially weakens the interchain repulsion, making the hydrophobic segments more prone to association. At the same time, the acidic environment makes the molecular chain conformation more extended, which is favorable for hydrophobic groups to approach each other, thereby reducing the critical association concentration.

As shown in **Fig. 4(c)** and **(d)**, after adding 200 mg/L of the betaine-type surfactants EDCB and EDSB to 20 wt% HCl, the critical association concentrations of MFAT further decrease. With the assistance of EDCB, the first and second critical association concentrations decrease to 922.3 mg/L and 1812.7 mg/L, respectively. With the assistance of EDSB, they decrease to 903.1 mg/L and 1643.1 mg/L, respectively. This indicates that betaine surfactants can form mixed micelles with MFAT hydrophobic chains, promoting intermolecular association of the polymer through hydrophobic–hydrophobic interactions and electrostatic interactions, so that the associating network can form at a lower concentration. The decrease caused by EDSB is greater than that caused by EDCB, indicating that sulfobetaine has a stronger synergistic effect with MFAT, which is related to the stronger polarity and charge characteristics of its sulfonic group, favoring the formation of a more stable mixed association structure.

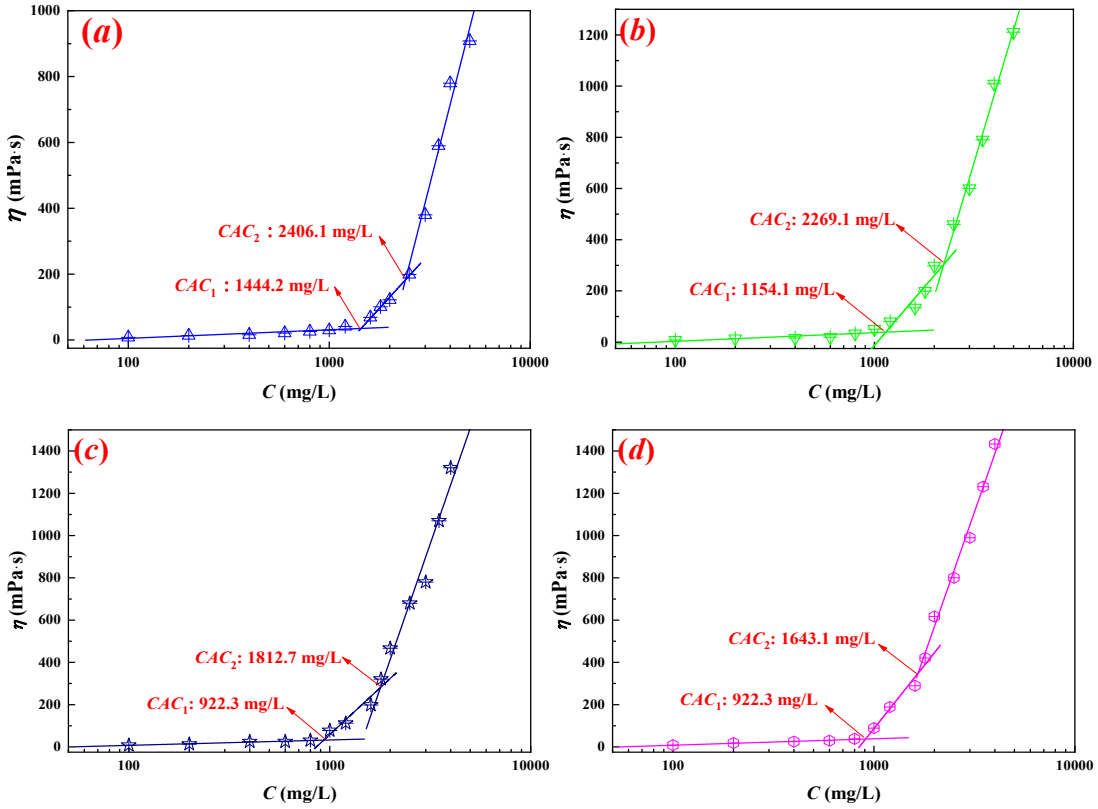


Fig. 4 Critical association concentration test results: (a) in pure water; (b) in 20 wt%HCl; (c) 20 wt%HCl + 200 mg/L EDCB; (d) 20 wt%HCl + 200 mg/L EDSB

3.3 Gelled acid system test

An acid fluid system directly thickened by a polymer is a gelled acid [27, 28]. In this work, 0.6 wt%MFAT was used as the thickener to thicken a 20% HClsystem, and 200 mg/LEDCB and EDSB were respectively added to assist thickening, so as to compare the performance of different gelled acid formulations.

3.3.1 Rheological properties of gelled acid

A gelled acid with an HCl concentration of 20 wt% was prepared using 0.6 wt%MFAT, and 200 mg/LEDCB and EDSB were respectively added to assist thickening. The rheological properties were tested, and the results are shown in Fig. 5. **Fig. 5(a)** shows the thixotropy test results of the three fluids. A three-stage shear rate protocol was adopted: (a) linear increase from 0 to 100 s^{-1} over 10 min; (b) constant shear at 0 $s^{-1}$for 3 min; and (c) linear decrease from 100 to 0 s^{-1} over 10 min.

The shear stress first increased to a maximum value with increasing shear rate and then decreased back to the origin, forming a typical hysteresis loop. The area enclosed by the hysteresis loop represents the energy required to disrupt the fluid structure; a

larger area indicates greater structural stability and slower recovery. This thixotropic behavior arises from the temporal decoupling between the internal structural reorganization of the polymer and the applied shear field, as well as chain entanglement in the macromolecular network [23, 29-30].

As shown in **Fig. 5(a)**, the gelled acid system thickened only by MFAT has the smallest hysteresis loop area. After adding betaine surfactants, the hysteresis loop area increases, and the system with 200 mg/L EDSB has the largest hysteresis loop area. This indicates that EDSB enables MFAT to construct a denser three-dimensional network structure in a strongly acidic environment. The mechanism is that betaine surfactant molecules can form mixed micelles with MFAT hydrophobic chains, increasing the density of physical crosslinking points; at the same time, the electrostatic interaction between the surfactant and cationic groups can enhance the synergistic effect between molecular chains, making the network structure recover more slowly after shear disruption, thus exhibiting stronger thixotropy.

Fig. 5(b) shows the viscoelasticity test results of the gelled acid. Overall, the elastic modulus $G'$of the three acid fluids is higher than the viscous modulus G'', indicating that the systems are dominated by elastic network structures [31-33]. Among them, the MFAT strong acid solution with 200 mg/LEDSB exhibits the best viscoelasticity, with the highest plateau modulus $G_0$of 60.38 Pa; the system with 200 mg/L EDCB has a plateau modulus G_0 of 51.56 Pa; and the MFAT strong acid solution without VES has a plateau modulus G_0 of 42.16 Pa. The increase in plateau modulus indicates that betaine surfactants and MFAT synergistically form a stronger three-dimensional network, enabling the acid fluid to maintain better structural stability under high temperature and high shear conditions. The EDSB system is superior to the EDCB system, indicating that sulfobetaine has stronger hydrophobic association and electrostatic synergy with MFAT.

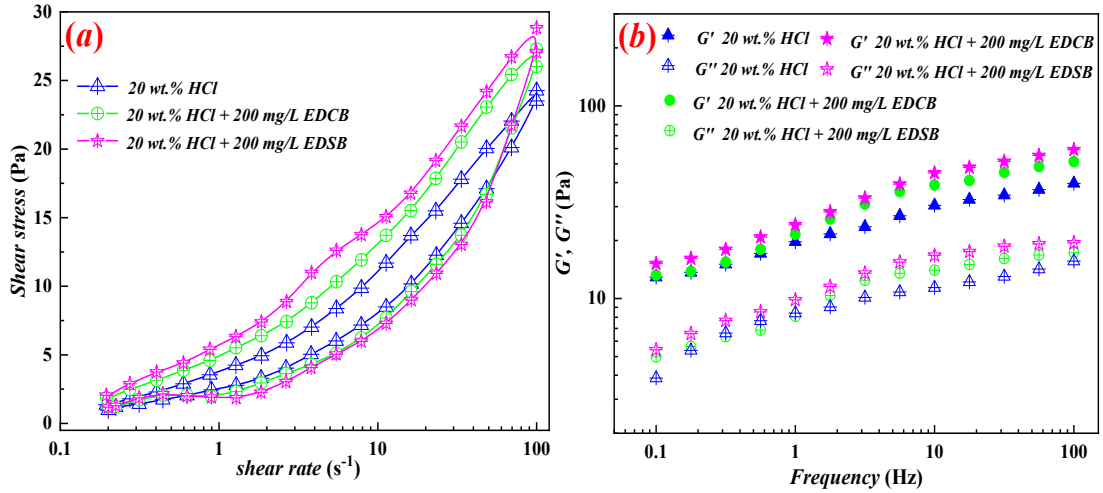


Fig. 5 Rheological evaluation of MFAT solution: (a) thixotropy; (b) viscoelasticity

3.3.2 Temperature and shear resistance

Fig. 6 shows the temperature and shear resistance test results of the three gelled acid systems at $160°C$ and $170\ s^{-1}$. As shown in Fig. 6, after shearing at $160°C$ and $170\ s^{-1}$ for 120 min, the acid fluid system thickened only with 0.6 wt% MFAT has a residual apparent viscosity of $29.8\ mPa \cdot s$; after adding 0.02 wt% EDCB and 0.02 wt% EDSB, the residual apparent viscosity after shearing increases to $34.5\ mPa \cdot s$ and $47.1\ mPa \cdot s$, respectively.

The above results indicate that MFAT itself has good temperature and shear resistance under high-temperature and strongly acidic conditions, which is related to the reversibility of its hydrophobic associating network and the acid resistance stability of its cationic groups. After adding betaine surfactants, the temperature resistance of the system is further improved. The mechanism is that surfactants form mixed micelles with MFAT hydrophobic chains, increasing the thermal stability of physical crosslinking points; at the same time, cationic–anionic electrostatic interactions can delay the dissociation of the network structure at high temperature, enabling the system to maintain relatively high viscosity after long-term high-temperature shearing. The improvement caused by EDSB is greater than that caused by EDCB, indicating that sulfobetaine has better synergy with MFAT under high-temperature and strongly acidic conditions.

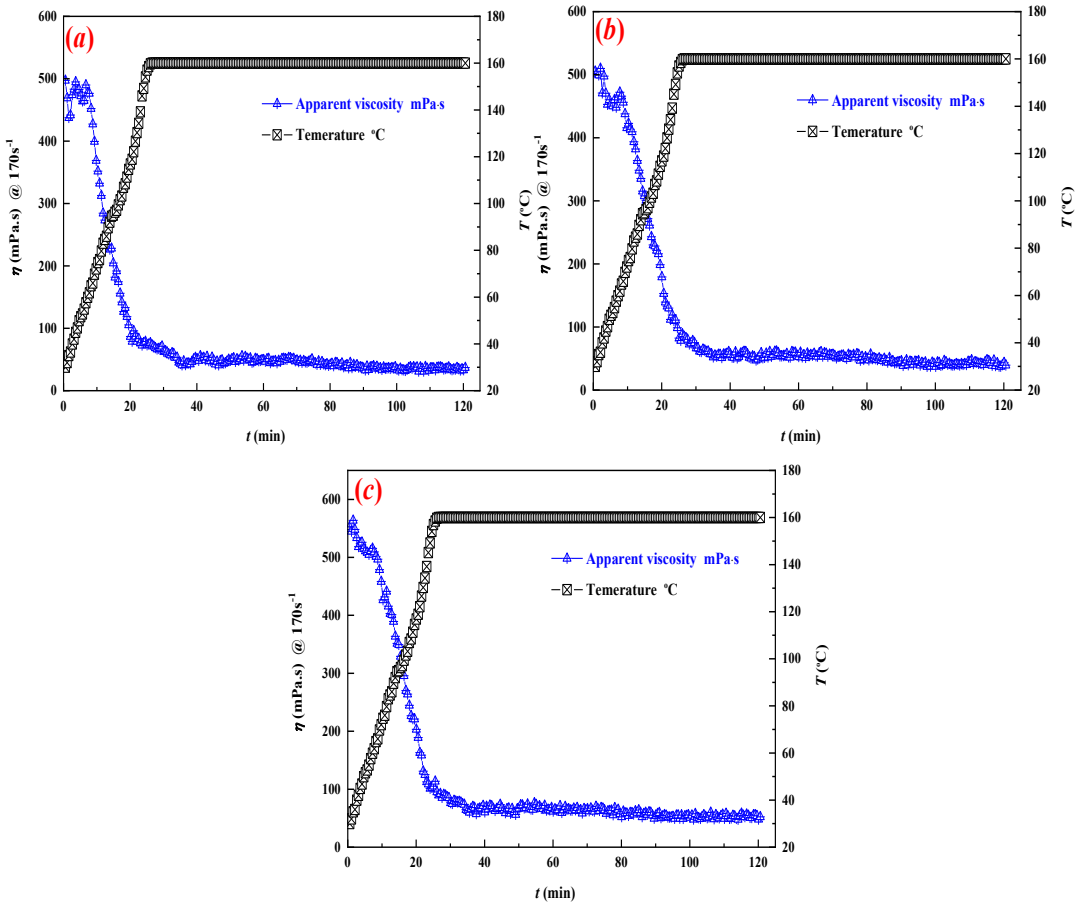


Fig. 6 Temperature and shear resistance tests of three gelled acid systems at 160°C and 170 s^{-1}: (a) 0.6 wt%MFAT + 20 wt%HCl; (b) 0.6 wt%MFAT + 20 wt%HCl + 0.02 wt%EDCB; (c) 0.6 wt%MFAT + 20 wt%HCl + 0.02 wt% EDSB

3.3.3 Retardation performance

Fig. 7(a) shows the static dissolution rates of 20wt% blank hydrochloric acid, gelled acid without VES, and gelled acid systems with VES assistance on carbonate rock samples. As the temperature increases from 60°C to 160°C, the acid dissolution rate of each system increases, and the increase amplitude becomes larger with increasing temperature. **Fig. 7(b)** shows the variation of the retardation rate of the three acid fluid systems with temperature. It can be seen that the retardation rates of the three acid fluid systems all increase with increasing temperature. This is because the dissolution rate of blank 20 wt%hydrochloric acid on carbonate rock increases sharply with increasing temperature, while the gelled acid system, due to its higher viscosity, has a more significant inhibitory effect on H^+ mass transfer, so its retardation rate is relatively improved.

Comparing the three gelled acid systems, the gelled acid system with VES assistance has better retardation performance than the gelled acid thickened only with MFAT. The

mechanism is that the associating network formed by the synergy of VES and MFAT is denser, increasing the resistance to H^+ diffusion toward the rock surface; at the same time, the highly viscous elastic network can form a certain adsorption layer on the rock surface, further reducing the acid–rock reaction rate [34, 35]. Therefore, the MFAT/VES composite gelled acid has better retardation performance at high temperature, which is conducive to achieving deep acid penetration.

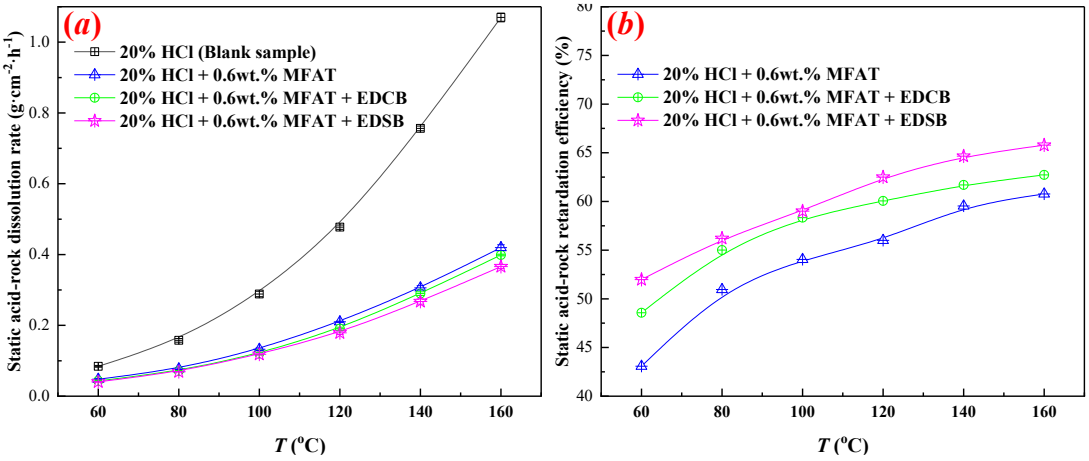


Fig. 7 Retardation effect evaluation: (a) static dissolution rate at different temperatures; (b) retardation rate at different temperatures

3.4 Delayed crosslinking characteristics

The significance of delayed crosslinked acid is to allow the acid fluid to crosslink after entering the formation, thereby greatly increasing viscosity and achieving retardation, while avoiding large friction caused by high-viscosity fluid in the tubing. In this work, an organic zirconium crosslinker was used to evaluate the crosslinking effect of MFAT.

3.4.1 Crosslinking time and effect

The performance of the crosslinked acid system was evaluated by the crosslinking time, the hanging-lip state of the acid fluid system after crosslinking and gelation, and the residual viscosity after temperature and shear resistance testing at 160°C and 170 s^{-1} for 2 h. The results are shown in **Table 2** and **Fig. 8**.

Table 2 Effect of crosslinker dosage on crosslinked acid performance in 20 wt%HCl environment

Dosage/%	Time of crosslinking/s	Hang-lip	Residual viscosity/mPa · s
0.6	318	bad	43.1

Dosage/%	Time of crosslinking/s	Hang-lip	Residual viscosity/mPa · s
0.8	239	excellent	79.3
1.0	157	excellent	89.2
1.2	101	brittle	70.3
1.4	78	brittle	60.1

As the dosage of organic zirconium crosslinker increases from 0.6% to 1.4%, the crosslinking time gradually shortens, and the residual viscosity after temperature and shear resistance testing first increases and then decreases. Among them, when the crosslinker dosage is 1.0%, the temperature and shear resistance performance is the best, and the gel formed after crosslinking has the best hanging-lip property. The reason is that an appropriate amount of crosslinker can form a uniform coordination crosslinking network with the carboxyl, amide, and sulfonic groups on the MFAT molecular chain, giving the gel relatively high viscosity and elasticity. When the crosslinker dosage is excessive, the crosslinking density is too high, the network structure becomes too rigid and brittle, and it is prone to fracture under high-temperature shear, resulting in a decrease in residual viscosity. Therefore, 1.0%is the optimal dosage of organic zirconium crosslinker.

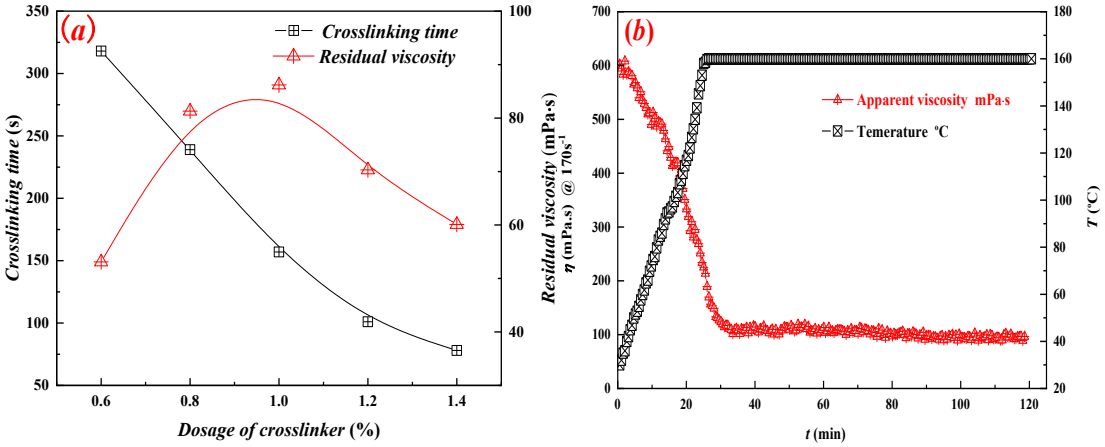


Fig. 8 Crosslinked acid effect evaluation: (a) effect of crosslinker dosage on crosslinking time and residual viscosity after temperature and shear resistance; (b) temperature and shear resistance test results of the gel corresponding to 1.0%

crosslinker

3.4.2 Retardation effect

After the crosslinked acid forms a gel, the three-dimensional network structure becomes denser, and the inhibitory effect on H^+ mass transfer is better [34, 35]. As shown in **Fig. 9(a),** the static dissolution rate of the gel acid formed after crosslinking on rock samples increases with increasing temperature, and the increase amplitude gradually becomes larger, but the overall increase amplitude is much lower than that of blank hydrochloric acid. As shown in **Fig. 9(b)**, as the temperature increases, the retardation effect gradually improves, and the retardation rate is higher than the best retardation rate of the gelled acid in **Fig. 7**.

The mechanism is that the organic zirconium crosslinker forms coordination crosslinks with carboxyl, amide, and other groups in MFAT, transforming the system from a physical association network to a chemical–physical synergistic crosslinking network, and significantly improving the network density and structural strength. This dense network can effectively prolong the diffusion path of H^+, reducing the acid–rock reaction rate. At the same time, the crosslinked gel can still maintain relatively high viscosity at high temperature, thus exhibiting excellent retardation performance at 160°C, which is conducive to deep penetration acidizing of high-temperature carbonate reservoirs.

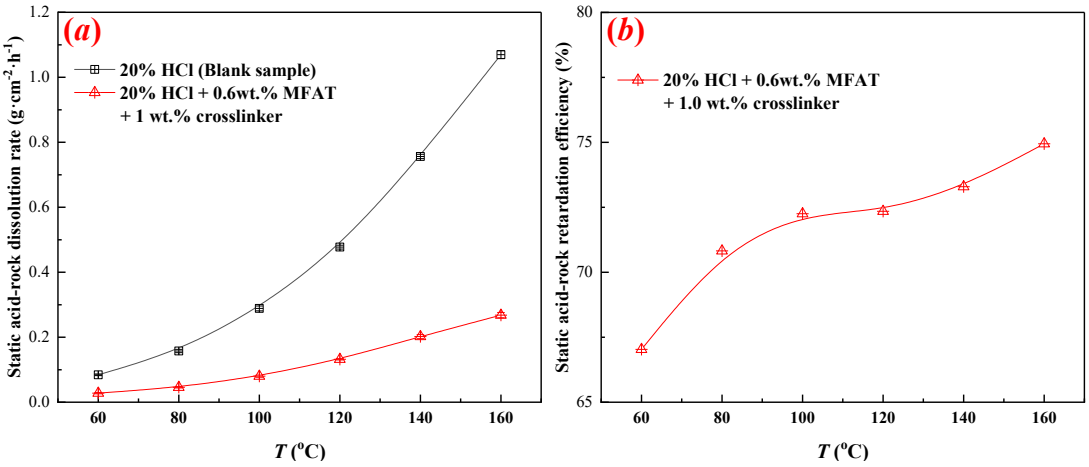


Fig. 9 Retardation effect of the crosslinked acid system in the optimal crosslinking state: (a) variation of static dissolution rate with temperature; (b) variation trend of retardation effect with temperature

3.5 Drag-reducing acid

First, the optimal dosage of MFAT as a drag reducer was screened. The test was conducted at a displacement of 30 L/min, and the results are shown in **Fig. 10(a)**. As

the MFAT dosage increases from 0.05 wt% to 0.2 wt%, the drag reduction rate gradually increases and reaches a maximum value; with a further increase in MFAT dosage, the drag reduction rate begins to decrease. This is because when the MFAT concentration is too high, the overall viscosity of the system increases, and the along-path viscous resistance increases, offsetting the inhibitory effect of the polymer on turbulence.

A 20% HCl drag-reducing acid was prepared using 0.2 wt% MFAT as the drag reducer, and 200 mg/L EDCB and EDSB were respectively added to form three drag-reducing acid systems. The drag reduction rates at different displacements were investigated, and the results are shown in **Fig. 10(b)**. After adding VES, the drag reduction effect is significantly improved, and EDSB has the best improvement effect. This is because the addition of VES enhances the viscoelasticity of the system, resulting in better elastic drag reduction; at the same time, VES and MFAT form a mixed association structure, which can improve the shear resistance and elastic recovery ability of the polymer network in a turbulent field, thereby more effectively inhibiting the development of turbulent vortices and reducing friction.

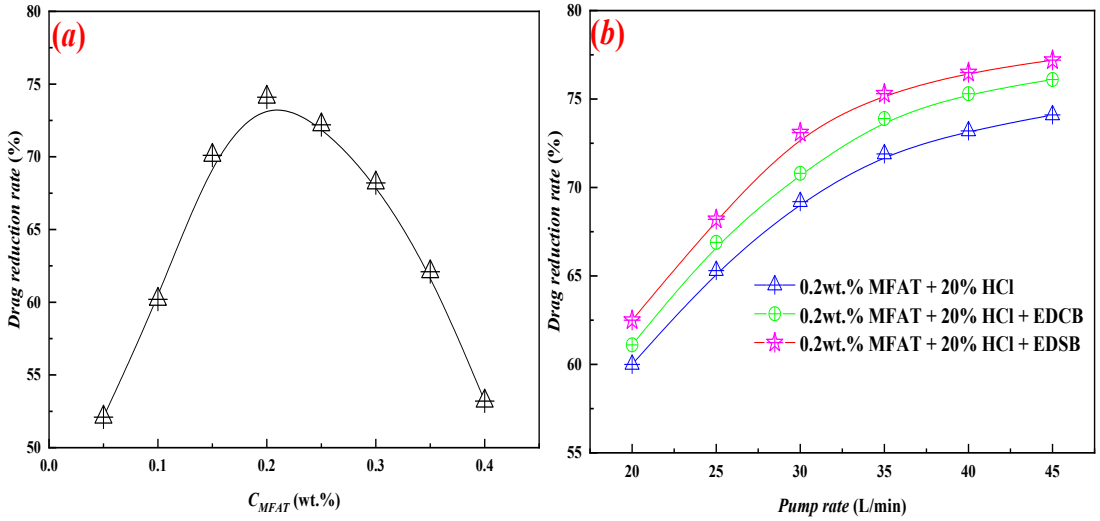


Fig. 10 Evaluation of MFAT as an acid drag reducer: (a) effect of MFAT concentration on drag reduction rate at a displacement of 30 L/min; (b) variation of drag reduction rate with displacement for three formulation systems at 0.2 wt% MFAT dosage

3.6 Viscosity-variation acid stabilizer

VES clean diverting acid has good application performance, but the system constructed by small molecules has poor temperature resistance. The MFAT developed in this work can also serve as a stabilizer for VES diverting acid to improve its temperature resistance.

3.6.1 Viscosity-variation effect

First, a commercially available diverting acid SDA was selected to study the viscosity-variation effect after adding 0.1 wt% MFAT. The results are shown in **Fig. 11(a)**. The results show that the addition of MFAT has no obvious effect on the viscosity-variation trend. Both systems exhibit the highest viscosity when HCl is consumed to 5 wt% by $Ca(OH)_2$. At the same time, after adding 0.1 wt% MFAT, the highest viscosity is increased, which provides a guarantee for temperature and shear resistance. **Fig. 11(b)** shows the variation of the viscosity of the spent acid of SDA diverting acid and the diverting acid with 0.1 wt% MFAT with temperature. It can be seen that after adding 0.1 wt% MFAT, the temperature resistance of the spent acid of the diverting acid is greatly improved.

The mechanism is that after the acid–rock reaction of VES diverting acid, surfactant micelles transform from spherical to wormlike, forming a high-viscosity spent acid and thus achieving diverting plugging. However, small-molecule VES micelles are easily dissociated at high temperature, leading to a decrease in viscosity. After MFAT is added, its long hydrophobic chains can undergo hydrophobic association with the hydrophobic tails of VES, and its cationic groups can undergo electrostatic interaction with anionic or amphoteric surfactants, forming more stable mixed micelles and a three-dimensional network, thereby significantly improving the temperature resistance and structural stability of the spent acid.

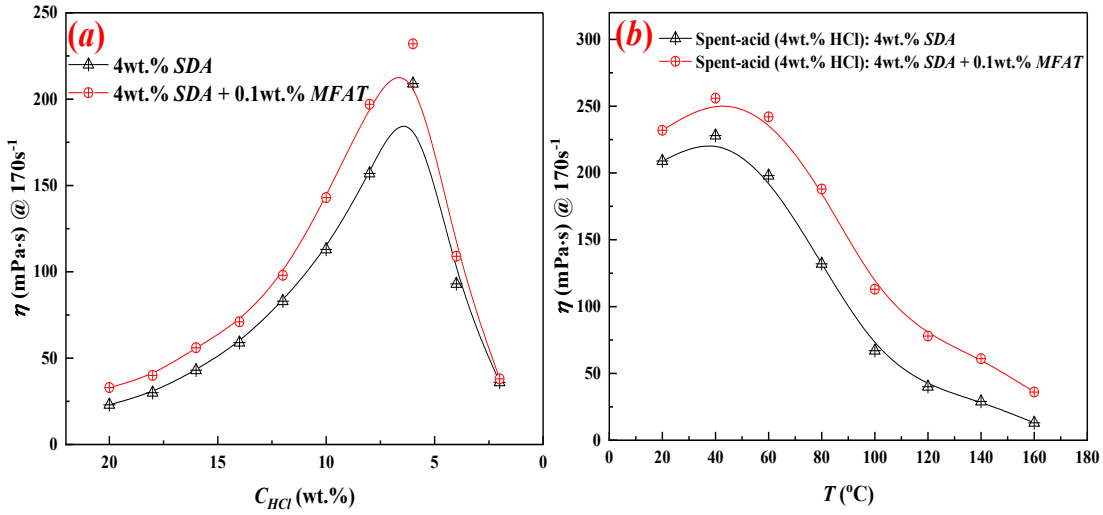


Fig. 11 Diverting acid effect evaluation: (a) viscosity-variation effect; (b) variation of apparent viscosity of high-viscosity spent acid with temperature

3.6.2 Viscoelasticity of diverting acid

The spent acid formed after the reaction of diverting acid with carbonate rock has

increased viscosity, achieving diversion, and is characterized by good viscoelasticity, thereby plugging macropores. **Fig. 12** shows the viscoelasticity of the high-viscosity spent acid before and after adding 0.1 wt%MFAT to SDA diverting acid. After adding MFAT as a stabilizer, the viscoelasticity is significantly improved, and both the elastic modulus $G'$and the viscous modulus $G''$are increased; after adding 0.1 wt% MFAT, the plateau modulus G_0increases from 35.3 Pa to 45.6 Pa.

The increase in plateau modulus indicates that MFAT and VES synergistically form a stronger three-dimensional network structure, giving the spent acid higher plugging strength and more stable viscoelasticity in high-permeability macropores. The mechanism is that the hydrophobic association between the hydrophobic chains of MFAT and VES micelles, as well as the electrostatic interaction between cationic groups and betaine surfactants, jointly enhance the crosslinking density and thermal stability of the micelle network, thereby improving the plugging ability of the diverting acid at high temperature.

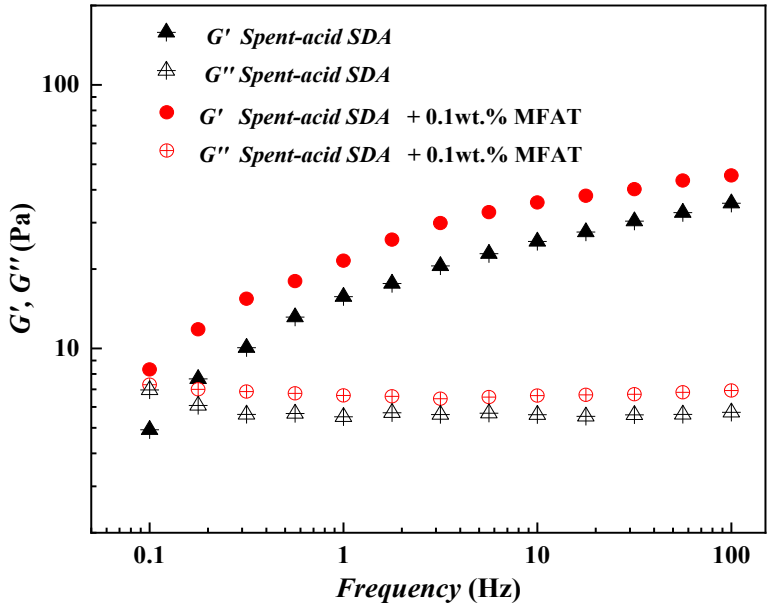


Fig. 12 Viscoelasticity test of high-viscosity spent acid before and after adding 0.1 wt%MFAT to SDA diverting acid

To evaluate the actual diversion acidizing effect of the diverting acid in heterogeneous carbonate reservoirs, parallel displacement experiments were conducted using high- and low-permeability carbonate cores at 160°C to simulate formation heterogeneity. The results are shown in **Fig. 13**.

Fig. 13(a) shows the parallel core displacement results of conventional hydrochloric acid. During the entire displacement process, the displacement pressure basically does

not change significantly, indicating that conventional hydrochloric acid mainly flows along the high-permeability core, and the low-permeability core is not effectively stimulated. This is because conventional hydrochloric acid has low viscosity and a fast acid–rock reaction rate. After entering the high-permeability core, the acid rapidly reacts with the rock and is consumed, making it difficult to form effective plugging in the high-permeability channel, and thus unable to force subsequent acid to divert into the low-permeability core [18-20].

Fig. 13(b) shows the parallel core displacement results of gelled acid. Compared with conventional hydrochloric acid, the displacement pressure of gelled acid is increased to a certain extent and then gradually decreases. This indicates that gelled acid, due to its higher viscosity, can delay the acid–rock reaction to a certain extent and increase the displacement pressure, but its viscoelasticity is limited, and it cannot form a stable plugging structure in the high-permeability core, so the diversion effect is still not significant.

Fig. 13(c) and (d) show the parallel core displacement results of SDA diverting acid and SDA diverting acid with MFAT stabilizer, respectively. Both systems generally exhibit a process in which the displacement pressure first increases, reaches the breakthrough pressure, and then decreases. The pressure increase stage corresponds to the acid entering the high-permeability core and reacting with the rock, during which the viscosity of the spent acid gradually increases and forms a high-viscosity micelle structure, temporarily plugging the high-permeability channel and causing the displacement pressure to rise. When the pressure reaches the breakthrough pressure, the subsequent acid is forced to enter the low-permeability core, achieving acid diversion. The higher the pressure increase, the greater the plugging strength of the high-permeability channel and the better the diversion effect.

The breakthrough pressure of the SDA diverting acid without MFAT is 3.97 MPa; after adding 0.1 wt% MFAT, the breakthrough pressure increases to 5.31 MPa. This indicates that MFAT can significantly enhance the plugging strength and diversion ability of SDA diverting acid at 160°C. The mechanism is that the long hydrophobic chains of MFAT can undergo hydrophobic association with VES micelles, and the cationic groups can undergo electrostatic interaction with betaine surfactants, forming a more stable mixed micelle network, thereby improving the viscoelasticity and structural strength of the high-temperature spent acid, making the temporary plugging

of the high-permeability channel more firm and forcing more acid to enter the low-permeability core.

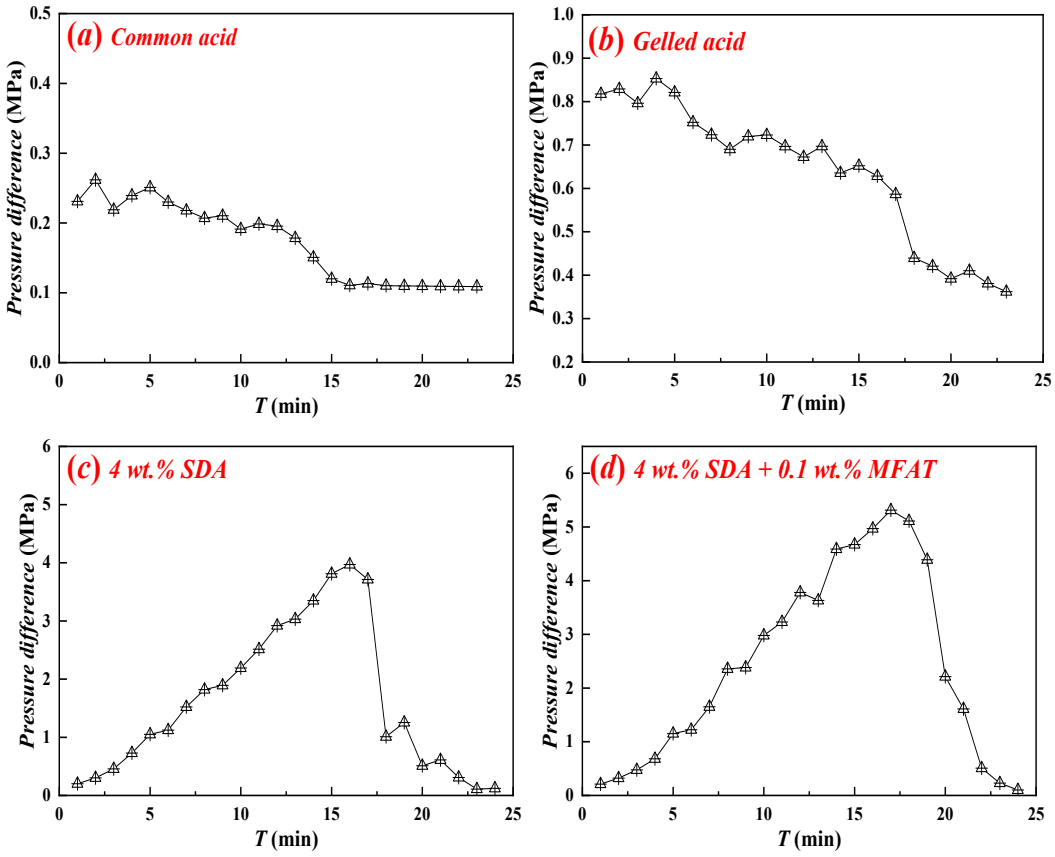


Fig. 13 Parallel core displacement process: (a) common acid; (b) gelled acid; (c) SDA diverting acid without MFAT; (d) SDA diverting acid with 0.1 wt%MFAT

After parallel core displacement, the acidizing stimulation effect of the cores was evaluated, and the results are shown in **Table 3**.

As shown in **Table 3**, after parallel displacement experiments with common hydrochloric acid and gelled acid, the permeability improvement ratios $(K_1/K_0)$of the low-permeability cores are 1.083 and 2.034, respectively, indicating that common hydrochloric acid has basically no stimulation effect on the low-permeability core, and gelled acid, although somewhat improved, still has limited diversion ability. After parallel displacement experiments with SDA diverting acid and MFAT-assisted SDA diverting acid, the permeability improvement ratios of the low-permeability cores are 8.53 and 12.63, respectively, indicating that both have good diversion acidizing effect. Among them, the MFAT-assisted SDA diverting acid can increase the permeability improvement ratio of the low-permeability core by nearly 50%, significantly superior to the SDA diverting acid without MFAT.

The above results indicate that MFAT can greatly improve the diversion performance

of SDA diverting acid under high-temperature conditions. The mechanism can be summarized as follows: on the one hand, MFAT enhances the thermal stability of the VES micelle network through hydrophobic association and electrostatic interaction, enabling the spent acid to maintain relatively high viscosity and viscoelasticity at high temperature; on the other hand, the high-viscosity spent acid formed by the synergy of MFAT and VES can form a stronger temporary plugging structure at the pore throats of the high-permeability core, increasing the breakthrough pressure and forcing subsequent acid to enter the low-permeability core, thereby significantly improving the acidizing stimulation effect of heterogeneous reservoirs. Therefore, MFAT, as a VES diverting acid stabilizer, has good application prospects in high-temperature heterogeneous carbonate diversion acidizing.

Table 3 Permeability changes of cores before and after parallel core experiments

Core#	Acid	K_0(mD)	K_1(mD)	K_1/K_0	T(°C)
1	common acid	5.182	401.78	77.53	160
2		0.573	0.621	1.083	
3	gel acid	6.115	489.31	80.01	160
4		1.078	2.193	2.034	
5	4% SDA	5.102	587.17	115.02	160
6		0.531	4.531	8.53	
7	4% SDA + 0.1% MFAT	4.518	378.31	83.73	160
8		1.037	13.106	12.63	

4 Conclusions

(1) A zwitterionic pentacopolymer hydrophobic associating thickener MFAT was designed and synthesized from AM, AA, AMPS, DMDAAC, and DCGM. It contains amide, carboxyl, sulfonic, quaternary ammonium cationic, and long hydrophobic chains, enabling a physical crosslinking network through hydrophobic association,

electrostatic interaction, and hydrogen bonding in strongly acidic and high-ionic-strength environments. Structural characterization confirmed successful synthesis, with a viscosity-average molecular weight of 8.43×10^6 g/mol.

(2) MFAT shows good thickening ability in 20% HCl as a gelled acid thickener. Its critical association concentrations in 20% HCl are lower than in pure water, and EDCB and EDSB further reduce these values. The MFAT/betaine composite gelled acid exhibits excellent thixotropy and viscoelasticity, with a residual viscosity of 29.8 mPa·s after shearing at 160 °C and 170 s^{-1} for 120 min, increasing to 34.5 and 47.1 mPa·s with EDCB and EDSB, respectively, and a retardation rate above 65%.

(3) MFAT and organic zirconium crosslinker can construct a delayed crosslinked acid system. At a crosslinker dosage of 1.0%, the crosslinking time is 157 s, and the residual viscosity after shearing at 160 °C and 170 s^{-1} for 2 h reaches 89.2 mPa·s, with a retardation rate above 75%.

(4) MFAT can serve as a drag reducer for 20% HCl. At 0.2 wt%, it shows the best drag reduction effect, and adding EDCB or EDSB significantly improves performance, with the EDSB system achieving a drag reduction rate above 75%.

(5) MFAT significantly improves the temperature resistance and diversion acidizing effect of VES diverting acid. After adding 0.1 wt% MFAT, the breakthrough pressure at 160 °C increases from 3.97 to 5.31 MPa, and the permeability improvement ratio of the low-permeability core increases from 8.53 to 12.63, an increase of nearly 50%.

(6) In summary, MFAT, as a multifunctional acid thickener, can simultaneously serve as a gelled acid thickener, crosslinked acid thickener, drag reducer, and VES diverting acid stabilizer in high-temperature carbonate acidizing. The synergistic effect of its cationic groups, sulfonic groups, and long hydrophobic chains enables excellent performance in strongly acidic, high-temperature, and high-ionic-strength environments, offering important theoretical significance and engineering application value for simplifying high-temperature acidizing fluid formulations and improving carbonate reservoir stimulation.

Acknowledgement

No

Data Availability declaration

No datasets were generated or analysed during the current study.

Ethics declarations

Our research does not include human or animal subjects.

Funding statement

References

[1] Wang, M.; Zhou, W.; Li, S.; Wu, W. Simulated Investigation in Wormhole Expansion Law of Gelling Acid Etching and Its Influencing Factors in Deep Carbonate Reservoirs. *Gels* **2022**, 8 (8), 470. DOI: 10.3390/gels8080470.

[2] Yue, G.; Wang, G.; Ma, F.; et al. Research on the Mechanism of Acidizing the Carbonate Gaoyuzhuang Reservoir, North China: Insights from Field Experiments and Numerical Simulations. *Geothermics* **2025**, 133, 103460. DOI: 10.1016/j.geothermics.2025.103460.

[3] Sui, Y.; Cao, G.; Guo, T.; Li, Z.; Bai, Y.; Li, D.; Zhang, Z. Development of Gelled Acid System in High-Temperature Carbonate Reservoirs. *Journal of Petroleum Science and Engineering* **2022**, 216, 110836. DOI: 10.1016/j.petrol.2022.110836.

[4] Wang, C.; Zhao, L.; He, B.; Zhang, X.; Mmbuji, A. O. Comparative Analysis of Matrix-Retarded Acidizing Methods for Tight Carbonate Reservoirs: Gelled Acid, Micro-Emulsified Acid, and Foamed Acid. *Frontiers in Earth Science* **2023**, 10, 1060213. DOI: 10.3389/feart.2022.1060213.

[5] Ji, S. W.; Zheng, Y. C.; Zhang, Y.; et al. Machine Learning-Based Evaluation of Acidizing Effectiveness and Optimization of Acidizing Parameters for Carbonate Gas Reservoir Horizontal Wells. *Thermal Science* **2025**, 29 (2 Part A), 1043–1048. DOI: 10.2298/TSCI2502043J.

[6] Gomaa, A. M. Proper Design of Polymer-Based In-Situ Gelled Acids to Improve Carbonate Reservoir Productivity. *SPE Annual Technical Conference and Exhibition* **2010**. DOI: 10.2118/141123-STU.

[7] Taylor, K. C.; Nasr-El-Din, H. A. Laboratory Evaluation of In-Situ Gelled Acids for Carbonate Reservoirs. *SPE Journal* **2003**, 8 (4), 426–434. DOI: 10.2118/71694-MS.

[8] Nasr-El-Din, H. A.; Taylor, K. C.; Al-Hajji, H. H. Propagation of Cross-Linkers Used in In-Situ Gelled Acids in Carbonate Reservoirs. DOI: 10.2118/75257-MS.

[9] Lan, X.; Liu, P.; Pan, D.; et al. Strongly Associating Dual-Network High-Temperature-Resistant Crosslinked Acid Based on Dual-Modified Nano-SiO2. *Oilfield Chemistry* **2025**, 42 (4), 614–621. DOI: 10.19346/j.cnki.1000-4092.2025.04.006. (in Chinese)

[10] Yan, Y.; Wang, Y.; Hou, F.; et al. Preparation and Performance Evaluation of a

High-Temperature-Resistant Deep-Penetrating Organic Delayed Crosslinked Acid Composite System. *Applied Chemical Industry* **2024**, 53 (7), 1515–1518, 1522. DOI: 10.16581/j.cnki.issn1671-3206.2024.07.008. (in Chinese)

[11] Hu, J.; Chen, T.; Cheng, F.; et al. Preparation and Application of a Hydrophobically Associating Crosslinked Acid Thickener. *Oilfield Chemistry* **2020**, 37 (3), 403–408. DOI: 10.19346/j.cnki.1000-4092.2020.03.005. (in Chinese)

[12] Liang, S.; Wang, Y.; Li, D.; et al. Construction and Performance Evaluation of a Temperature-Resistant Acidic Slickwater System. In *Proceedings of the 2023 International Conference on Oil and Gas Field Exploration and Development*, Vol. II; China University of Geosciences (Wuhan), Xi'an Shiyou University, Shaanxi Petroleum Society, 2023; 764–772. DOI: 10.26914/c.cnkihy.2023.059513. (in Chinese)

[13] Yang, C.; Sui, S.; Jia, W.; et al. Acidic Slickwater System for Fracturing Calcium-Rich Shale Oil and Gas. *Drilling Fluid & Completion Fluid* **2020**, 37 (1), 116–120, 126. (in Chinese)

[14] Tian, W.; Du, J.; Li, Y.; Li, J. Study on the Impact of Viscoelastic Surfactants on the Reaction-Retarding Performance of Carbonate Reservoir Acidizing. *Processes* **2026**, 14 (5), 873. DOI: 10.3390/pr14050873.

[15] Fu, Y.; Li, L.; Jia, Y.; Wang, H.; He, T. Application of a New Integrated Variable-Viscosity Retarded Acid in Carbonate Reservoir Stimulation. *Journal of Physics: Conference Series* **2025**, 3048 (1), 012045. DOI: 10.1088/1742-6596/3048/1/012045.

[16] Mao, J.; Wang, C.; Yang, X.; Zhang, H.; Zhang, W.; Zhang, C.; Lin, C. Self-Diverting Acid System with Retarding Function for Heterogeneous Carbonate Reservoirs Stimulation. *Journal of Surfactants and Detergents* **2020**, 23 (4). DOI: 10.1002/jsde.12407.

[17] Zheng, N.; Zhu, J.; Yang, Z.; Li, X.; Chen, H.; Hao, S.; Qiao, L. Molecular Dynamics Simulation and Key Performance Study of VES Self-Diverting Acid System for Deep Carbonate Reservoirs. *Journal of Molecular Liquids* **2024**, 401, 124645. DOI: 10.1016/j.molliq.2024.124645.

[18] Al-Shargabi, M.; Davoodi, S.; Wood, D. A.; Ali, M.; Rukavishnikov, V. S.; Minaev, K. M. A Critical Review of Self-Diverting Acid Treatments Applied to Carbonate Oil and Gas Reservoirs. *Petroleum Science* **2023**, 20 (2). DOI: 10.1016/j.petsci.2022.10.005.

[19] Wu, J.; Nie, F. Quantitative Analysis of Heterogeneity Effects and Heat Transfer on Self-Diverting Acid Performance in Multi-Layered Carbonate Reservoirs. *Processes*

2026, 14 (13), 2106. DOI: 10.3390/pr14132106.
[20] Zhang, W.; Mao, J.; Yang, X.; Zhang, H.; Yang, B.; Zhang, Z.; Zhao, J. Development of a Stimuli-Responsive Gemini Zwitterionic Viscoelastic Surfactant for Self-Diverting Acid. *Journal of Surfactants and Detergents* **2019**, 22 (3). DOI: 10.1002/jsde.12267.
[21] Tian, J.; Mao, J.; Zhang, W.; Yang, X.; Lin, C.; Cun, M.; Mao, J.; Zhao, J. Application of a Zwitterionic Hydrophobic Associating Polymer with High Salt and Heat Tolerance in Brine-Based Fracturing Fluid. *Polymers* **2019**, 11 (12), 2005. DOI: 10.3390/polym11122005.
[22] Jian, C.; Yu, Y.; Yu, D.; et al. Synthesis and Evaluation of Salt Tolerant Delayed-Crosslinking Fracturing Fluid System in Ultra-Deep High Temperature Wells. *Colloid and Polymer Science* **2024**, 302 (10), 1591–1601. DOI: 10.1007/s00396-024-05296-1.
[23] Zhang, W.; Chen, Y.; Tian, J.; et al. Development of Polymer Powder-Based Multifunctional Variable-Viscosity Slickwater Systems Assisted by Viscoelastic Surfactants for Enhanced Unconventional Reservoir Fracturing. *Chemical Engineering Journal* **2025**, 523, 168356. DOI: 10.1016/j.cej.2025.168356.
[24] Yang, D.; Yang, B.; Ren, M.; Liu, Y.; Cao, H.; Jiang, Z.; Zhang, H. Construction of Fracturing Fluid with Excellent Proppant Transport Capacity Using Low Molecular Weight Hydrophobic Association Polymer and Surfactant. *Journal of Molecular Liquids* **2023**, 377, 121546. DOI: 10.1016/j.molliq.2023.121546.
[25] Zhang, W.; Zhang, Q.; Xia, T.; et al. Development and Study of a Salt Tolerance Gemini Cationic Viscoelastic Surfactant with Spacer of Neopentyl-Glycol Applied in Seawater-Based Clean Fracturing Fluid. *Colloid and Polymer Science* **2025,** 303, 547-561.
[26] Zhang, W.; Mao, J.; Yang, Y.; et al. The Development and Performance of a Gemini Viscoelastic Surfactant with Tricationic Groups Applied in Unconventional Oil and Gas Reservoir Stimulation. *ChemistrySelect* **2024**, 9 (23), e202400399. DOI: 10.1002/slct.202400399.
[27] Danican, S.; Gettemy, D. J.; Izundu, K.; et al. New Advances in Single-Phase Retarded Acids for Stimulating Carbonate Reservoirs. *SPE International Conference and Exhibition on Formation Damage Control* **2024**. DOI: 10.2118/217841-MS.
[28] Quan, H.; Li, H.; Huang, Z.; Dai, S.; Jiang, J. Copolymer MCJS as a Retarder of the Acid-Rock Reaction Speed for the Stimulation of Deep Carbonate Reservoirs. *Journal of Applied Polymer Science* **2014**, 132 (7), 41471. DOI: 10.1002/app.41471.

[29] Xu, Z.; Zhao, M.; Sun, N.; Meng, X.; Yang, Z. Delayed Crosslinking Gel Fracturing Fluid with Dually Crosslinked Polymer Network for Ultra-Deep Reservoir: Performance and Delayed Crosslinking Mechanism. *Colloids and Surfaces A: Physicochemical and Engineering Aspects* **2025**, 708, 135967. DOI: 10.1016/j.colsurfa.2024.135967.

[30] Wu, Y.; Yan, X.; Huang, Y.; Zhao, M.; Zhang, L.; Dai, C. Ultra-Deep Reservoirs Gel Fracturing Fluid with Stepwise Reinforcement Network from Supramolecular Force to Chemical Crosslinking. *Energy* **2024**, 293, 130632. DOI: 10.1016/j.energy.2024.130632.

[31] Zhang, W.; Wan, L.; Fan, Y.; et al. Construction and Mechanism Study of Clean N2 Foam Fracturing Fluid Stabilized by Viscoelastic Surfactant in Concentrated Brines for Unconventional Oil and Gas. *Journal of Molecular Liquids* **2023**, 390 (Part B), 123168. DOI: 10.1016/j.molliq.2023.123168.

[32] Feng, C.; Ma, X.; Jing, Z. Dynamic Proppant-Carrying Performance of VES-CO2 Foam Fracturing Fluid in the Pipeline and the Fracture. *Journal of Petroleum Science and Engineering* **2022**, 210, 110034. DOI: 10.1016/j.petrol.2021.110034.

[33] Zhang, W.; Yan, L.; Liu, Y.; Tang, X.; Guo, B.; Yang, Y.; Liu, Y.; Wang, C.; Mao, J.; Xiaojiang. Development and Evaluation of Salt-Tolerant Green Surfactant-Based Multifunctional Fracturing Fluids Prepared by Formation Brine. *ChemistrySelect* **2025**, 10 (28), e202502318. DOI: 10.1002/slct.202502318.

[34] Cui, B.; Rong, X.; Guo, B.; et al. Novel Nano Retarded Acid System Enables Highly Effective Stimulation of Carbonate Reservoirs. *International Petroleum Technology Conference* **2025**. DOI: 10.2523/IPTC-24874-MS.

[35] Chen, W.-H.; Liu, P.; Li, A.; Wang, H.; Du, J.; Jia, Y.; Chen, X.; Gu, H. Retarded Gelled Acid for High-Temperature Carbonate Reservoir Acidizing: Retardancy and Mechanism Study. *ACS Omega* **2025**. DOI: 10.1021/acsomega.4c11617.